Boundary-Layer Meteorol manuscript No.
(will be inserted by the editor)

Response of London's urban heat island to a marine air intrusion in an easterly wind regime

Charles Chemel · Ranjeet S. Sokhi

Submitted: 23 May 2011 / Revised: R1 2 December 2011, R1 2 February 2012

Abstract Numerical simulations are conducted using the Weather Research and Forecast (WRF) numerical model to examine the effects of a marine air intrusion (including a sea-breeze front), in an easterly wind regime on 7 May 2008, on the structure of London's urban heat island (UHI). A sensitivity study is undertaken to assess how the representation of the urban area of London in the model, with a horizontal grid resolution of 1 km, affects its performance characteristics for the near-surface air temperature, dewpoint depression, and wind fields. No single simulation is found to provide the overall best or worst performance for all the near-surface fields considered. Using a multilayer (rather than single layer or bulk) urban canopy model does not clearly improve the prediction of the intensity of the UHI but it does improve the prediction of its spatial pattern. Providing surface-cover fractions leads to improved predictions of the UHI intensity. The advection of cooler air from the North Sea reduces the intensity of the UHI in the windward suburbs and displaces

C. Chemel (✉) · R. S. Sokhi

National Centre for Atmospheric Science (NCAS), Centre for Atmospheric & Instrumentation Research (CAIR), University of Hertfordshire, College Lane, Hatfield, AL10 9AB, UK

e-mail: c.chemel@herts.ac.uk

it several kilometres to the west, in good agreement with observations. Frontal advection across London effectively replaces the air in the urban area. Results indicate that there is a delicate balance between the effects of thermal advection and urbanization on near-surface fields, which depend, inter alia, on the parametrization of the urban canopy and the urban land-cover distribution.

Keywords Numerical simulations · Sea breeze · Sensitivity experiments · Urban parametrization schemes · Urban heat island

1 Introduction

London is long known to develop a pronounced heat island (Chandler 1962), resulting primarily from the storage of heat in the urban fabric during the day and released during the night, the differences in thermal and radiative properties of the surface between urban and rural areas, and reduced evapotranspiration in urban areas (e.g., Oke 1982; Arnfield 2003). Under calm, clear and dry weather conditions, the difference in near-surface air temperature between a representative urban centre and rural location at a given time, referred to as the urban heat island (UHI) intensity hereafter, typically reaches several K during the night and can be negative during the day.

Although limited, several studies have reported observations of London's heat island. Analysis of differences in daily minimum and maximum air temperatures during 1959 between central London at Kensington and Wisley, a rural site on the south-west outskirts, indicated that values of minimum temperature most frequently differed by 0.8 K, with a median of 1.7 K and a maximum of 6.1 K (Chandler 1962). The area of highest temperatures (referred to as the thermal centre) was found to usually lie north-east of central London, reflecting the density of urban development (see Fig. 2b) and the displacement of the heat

island by prevailing light south-westerly winds. Watkins et al. (2002) measured the London UHI intensity for summer 1999, with the intensity reaching 7 K on some days and averaged 2.8 K in August. The nighttime intensity tended to decrease with the radial distance from the thermal centre. This thermal centre was found to be located in the City of London borough, which is characterized by tall buildings and high anthropogenic heat release. This finding is supported by the earlier surveys of London's heat island by Chandler (1962), which indicated that the thermal centre is most frequently located north-east of central London. While its location is usually well defined for calm, clear and dry nights, it can move by several kilometres in relation to shifts in wind direction and the presence of clouds (see, for instance, Kolokotroni and Giridharan 2008; Giridharan and Kolokotroni 2009).

As with the large majority of megacities in the world, London is located in a coastal area. On certain occasions cooler marine air is advected across London by a sea-breeze front (SBF) from the North Sea or the English Channel. SBFs develop mostly from late spring through the summer, when the surface of the land heats up more rapidly than that of the sea. Their characteristics depend not only on the differential heating but also on the large-scale weather conditions (e.g., Estoque 1962; Bechtold et al. 1991; Arritt 1993; Zhong and Takle 1993; Atkins and Wakimoto 1997). Anticyclonic conditions in the North Sea or Baltic Sea regions, leading to easterly winds, are most favourable to the development of SBFs around the English Channel and the southern North Sea (Sumner 1977). Such anticyclonic conditions tend to occur more frequently in spring than in summer when the sea surface is cooler.

Marshall (1950) described a SBF that originated at the east coast, traversed London, and penetrated 150 km inland under relatively weak (3 m s^{-1}) easterly winds. The SBFs that develop on the south coast can penetrate to over 100 km from the coast, although such deep penetration inland is not frequent (Simpson et al. 1977). Damato et al. (2003) analyzed the

occurence of SBFs around the English Channel and the southern North Sea during the warm season (between May and September) of 2000 and found that the inland penetration was usually in the range 20 – 40 km from the coast in southern England. No SBF was observed to cross the North Downs (see Fig. 1b). Hence, we may conclude that the arrival of such SBFs in London is scarce. The analysis also revealed a higher occurence of SBFs eastward along the English Channel but with a lesser inland penetration. The south-westward retreat of these SBFs was suggested to be the result of the convergence between the SBFs originating from the English Channel and the Thames Estuary. Similar cases of convergence were reported by Eastwood and Rider (1961), Findlater (1964) and Simpson et al. (1977).

Several studies have reported complex interactions between a SBF and UHI (see, for instance, Miller et al. 2003; Crosman and Horel 2010). Interestingly, most of these studies focused on the influence of urban areas on the evolution of the SBF, whose characteristics may be weakened or strengthened by interactions with the UHI. The presence of the UHI intensifies the SBF and delays its penetration inland (Yoshikado 1990, 1992; Kusaka et al. 2000; Freitas et al. 2007; Dandou et al. 2009). The speed of the SBF increases as the size of the urban area increases (Ohashi and Kida 2002). In addition, surrounding topographic features and complex coastline geometries can lead to complicated interactions between a SBF and UHI (Ohashi and Kida 2004; Lemonsu et al. 2006).

Less attention has been paid to the modulation of the UHI intensity by the advection of cooler marine air by the SBF and to the contribution of the SBF to boundary-layer ventilation in the urban area. Gedzelman et al. (2003) analyzed surface weather observations in the Greater New York City Metropolitan area for the years 1997 and 1998 and found that SBFs typically delay the UHI of New York City for several hours and displace it about 10 km inland during spring and summer. In a numerical modelling case study of a SBF in the New York City area, Thompson et al. (2007) found that the SBF had a large impact on

the transport and diffusion of passive tracer plumes. The study showed that the SBF not only changed the direction of plume motion but also redistributed the tracers in the vertical. As the SBF passed a release location, upward motion at the front, resulting in boundary-layer ventilation, led to a decrease in near-surface tracer concentration. After the passage of the SBF, tracers were released and confined into the shallow sea-breeze flow, increasing near-surface tracer concentration.

Thompson et al. (2007) also pointed out that the local effects of SBFs in an urban environment are sensitive to the level of urbanization. Detailed case studies of these effects in urban areas with heterogenous land cover are essential to investigate such sensitivity. In the present study, we use numerical simulations to examine the effects of a marine air intrusion (including a sea-breeze front), in an easterly wind regime on 7 May 2008, on the structure of London's UHI. The simulations are performed with the Weather Research and Forecast (WRF) numerical model (Skamarock et al. 2008) for multiple nested domains with the innermost domain covering London and its rural surroundings with a horizontal grid resolution of 1 km. In order to evaluate the model performance, we also investigate the sensitivity of the simulated near-surface air temperature, dewpoint depression and wind fields to the representation of the urban area of London in the model. In the next section, we detail the set-up of the model and the design of the numerical experiments, with the model evaluation presented in Sect. 3. The response of London's UHI to the marine air intrusion is analyzed in Sect. 4 and concluding remarks are given in Sect. 5.

2 Design of the numerical experiments

Numerical simulations are conducted for a case study of 7 May 2008, which presents relevant features (Bohnenstengel et al. 2011). The synoptic-scale surface pressure distribution

on this day exhibited a typical pattern for late spring, with an anticyclone located over northern Europe and extending between the British Isles and the Baltic States. As indicated in the Introduction, this situation is favourable to the development of SBFs around the English Channel and the southern North Sea (Sumner 1977). The sky was clear over south-east England.

The WRF model, version 3.2.1, was run on multiple grids using one-way nesting with the innermost domain covering London and its rural surroundings at a horizontal resolution of 1 km. Table 1 gives the spatial coverage and horizontal resolution of the nested grids used for the simulations. The domain covering the UK and the Republic of Ireland using a 4-km horizontal resolution (Domain 3) is displayed in Fig. 1a. The calculations were made on 53 vertical levels up to 50 hPa (about 20 km). The grid mesh was stretched along the vertical axis to accommodate a high vertical resolution close to the ground surface (i.e., 15 layers below 2000 m with the first layer approximately 5 m deep).

The simulations commenced on 6 May 2008 at 1200 UTC and were run for 42 h (i.e., until 8 May 2008 at 0600 UTC). Initial and lateral boundary conditions of the outer domain (Domain 1) were derived from the European Centre for Medium-Range Weather Forecasts (ECMWF) gridded analyses available every 6 h with a horizontal resolution of 0.5° on operational pressure levels up to 50 hPa for vertically distributed data, and surface and soil levels for land-surface and deep-soil data. The sea-surface temperature was prescribed at the initial time using the Real-Time Global, SST High-Resolution (RTG_SST_HR) analysis available daily at a resolution of 1/12°(Gemmill et al. 2007). A grid nudging technique (four-dimensional data assimilation, Stauffer and Seaman 1990) was employed for the outer domain during the first 6 h of simulation in order to spin-up the model by constraining the model towards the analyses. The first 6 h of simulation were discarded for the analysis.

Urban areas are no longer entirely subgrid-scale features when their horizontal extent is much larger than that of a few model grid cells. This is the case for the Greater London area (see Fig. 1b), which covers an area of more than 1500 km^2, in Domain 3 and Domain 4 using horizontal resolutions of 4 and 1 km, respectively. However, even a horizontal resolution of 1 km is still too coarse to resolve the (thermo-) dynamics of the flow in the urban canopy. Therefore, the urban canopy must be parametrized.

The urban canopy can be parametrized in numerical weather prediction (NWP) models and in general circulation models (GCMs) in a number of different ways (Masson 2006). Three urban parametrization schemes have been included as options in the WRF model since version 3.1 (see Chen et al. 2011, for a description of the integrated urban modelling system coupled to the WRF model, its evaluation, and applications): (i) a bulk parametrization scheme described by Liu et al. (2006), (ii) the single-layer urban canopy model (SLUCM) developed by Kusaka et al. (2001) and Kusaka and Kimura (2004), and (iii) the multi-layer urban canopy model developed by Martilli et al. (2002), called the building effect parametrization (BEP). The building energy model (BEM) coupled to BEP, developed by Salamanca and Martilli (2010), is also available as an option from the WRF model version 3.2 onwards. A sensitivity study was undertaken to assess how the parametrization of the urban canopy (i.e., the selection of one of the options mentioned above) and the categorization of the urban land cover in the model affect its performance characteristics for the near-surface air temperature, dewpoint depression, and wind fields. Results of this sensitivity experiment are reported in Sect. 3.

The land-surface energy budget was calculated using the community Noah land-surface model (Chen and Dudhia 2001). For a given grid cell, the sensible heat flux $\mathscr{H}$ is aggregated (i.e., weighted by its areal coverage), so that $\mathscr{H} = \mathscr{F}_n \mathscr{H}_n + \mathscr{F}_u \mathscr{H}_u$, where $\mathscr{F}_n$ and $\mathscr{H}_n$, and $\mathscr{F}_u$ and $\mathscr{H}_u$ are the fractional areas and sensible heat fluxes for natural (i.e., non-urban) and

urban surfaces, respectively. $\mathscr{H}_n$ is calculated by the Noah land-surface model, and $\mathscr{H}_u$ is calculated by the urban parametrization scheme. The latent heat flux, longwave radiation flux, albedo and emissivity are estimated in the same way. Land-cover types were assigned to the grid cells for Domain 1 and Domain 2 using the modified International Geosphere-Biosphere Programme (IGBP)/MODerate resolution Imaging Spectroradiometer (MODIS) 20-category 1-km resolution land-cover dataset, provided with the WRF preprocessing system. This dataset contains a single urban land-cover category, for which the urban fraction $\mathscr{F}_u$ was set to 95% (Chen and Dudhia 2001).

The bulk urban parametrization scheme uses only one urban land-cover category. For this urban parametrization scheme, the IGBP/MODIS urban land-cover category was also used for Domain 3 and Domain 4. In the standard version of the WRF model, the SLUCM, BEP and BEP + BEM urban parametrization schemes can either use a single urban land-cover category or the three urban land-cover classes of the 1992 National Land Cover Dataset (NLCD) for the United States, for which default parameter values for the schemes are provided with the model. These classes are defined as low-intensity residential, high-intensity residential and commercial/industrial/transportation including infrastructure, for which $\mathscr{F}_u$ is set in the WRF model to 0.5, 0.9 and 0.95, respectively (see Chen et al. 2011, for further details). The urban grid cells for Domain 3 and Domain 4 were mapped onto these three classes according to the fractional area that is built-up within each grid cell, which was derived from the Landsat-based 2000 Centre for Ecology and Hydrology (CEH) 25-m resolution land-cover dataset. The land covers used for the simulations (i.e., IGBP/MODIS and CEH + IGBP/MODIS) are illustrated in Fig. 2, and a summary of the different simulations that were performed is given in Table 2.

A ‘very’ high vertical resolution (say in the order of 5 m) is necessary in the urban canopy in order to obtain full advantage of the multilayer BEP model because it requires

several layers within the urban canopy (Martilli et al. 2002). In contast to BEP, the bulk urban parametrization scheme and SLUCM parametrize the urban canopy as a whole. Hence, for these two parametrization schemes, the first vertical layer depth was set to about 20 m (i.e., above the mean building height).

We used the non-local boundary-layer parametrization scheme developed by Bougeault and Lacarrère (1989), which can be used with the three urban parametrization schemes. The Monin-Obukhov surface-layer scheme was coupled to the community Noah land-surface model to provide surface forcing in terms of momentum, heat and moisture fluxes. Other physics options that we used include the Rapid Radiative Transfer Model for GCMs (RRTMG) radiation package (Iacono et al. 2008), the two-moment bulk microphysics parametrization scheme developed by Morrison et al. (2009) and the ensemble cumulus parametrization scheme introduced by Grell and Dévényi (2002) for the two grids with a horizontal resolution larger than 4 km (i.e., for Domain 1 and Domain 2). For the finer-resolved grids (i.e., for Domain 3 and Domain 4), convection was explicitly resolved.

3 Model evaluation

3.1 Observations

The monitoring sites used for the model evaluation are reported in Fig. 2. Site 1 (Westminster - Marylebone Road) is part of the London Air Quality Network (LAQN) while all the other sites are part of the UK Met Office Integrated Data Archive System (MIDAS) land-surface stations, including surface SYNOPtic observation (SYNOP) and METeorological Aviation Report (METAR) stations. The automated stations provide data for near-surface (2-m) temperature, (2-m) dewpoint depression, and (10-m) wind speed and direction, except the LAQN station that does not measure the dewpoint. Systematic errors for the data

from the UK Met Office MIDAS land-surface stations should have been accounted for by a proper calibration of station instrumentation (UK Meteorological Office 2006). For the LAQN station, air temperature, and wind speed and direction are routinely measured using a Campbell CSAT3 sonic anemometer, maintained to quality assurance procedures. These measurements are subjected to quality control before ratification.

3.2 Near-surface fields

The predicted values for the near-surface fields (2-m temperature, 2-m dewpoint depression, 10-m wind speed and 10-m wind direction) are compared to their observed counterparts. For the bulk and SLUCM urban parametrization schemes, the urban canopy is parametrized as a whole and the values for the predicted near-surface fields were inferred using the Monin-Obukhov similarity theory (see Kusaka et al. 2001; Kusaka and Kimura 2004; Liu et al. 2006). The multilayer BEP model includes several layers within the urban canopy, where the Monin-Obukhov similarity theory is not valid (e.g., Rotach 1993), so that the values for the near-surface fields were set equal to those of the lowest model level (see Martilli et al. 2002).

The mean bias (MB), mean absolute error (MAE) and hit rate (HR) are calculated for hourly mean near-surface fields for the simulations S1 to S7, considering all the sites, all the urban sites only, and all the rural sites only (see Table 3). These statistical metrics used for model evaluation have been suggested by Schlünzen and Sokhi (2008). For a set of N predicted values $\mathscr{P}_i$ of a variable $\mathscr{V}$ with their counterpart observed values $\mathscr{O}_i$, where i refers to a given time and location, MB, MAE and HR are defined as

$$MB = \frac{1}{N}\sum_{i=1}^{N}(\mathscr{P}_i - \mathscr{O}_i),\ MAE = \frac{1}{N}\sum_{i=1}^{N}|\mathscr{P}_i - \mathscr{O}_i|,\ \text{and}\ HR = \frac{1}{N}\sum_{i=1}^{N}(1,\ |\mathscr{P}_i - \mathscr{O}_i| \leq DA),$$

where DA is the desired accuracy for the variable $\mathscr{V}$. MB is used to describe the overall overestimation or underestimation by the modelling system, while MAE gives information on the average error. HR quantifies the fraction of the predicted values that agree with their counterpart observed values for a desired accuracy. Hereafter, we use the values for desired accuracy reported by Cox et al. (1998), namely 2 K for air temperature and dewpoint depression, 1 and 2.5 m s^{-1} for wind speed less than and greater than 10 m s^{-1}, respectively, and 30° for wind direction. These values were established by the United States Air Force (USAF) and Defence Special Weapons Agency (DSWA) for mesoscale model applications over five very different regions of the world and during different seasons of the year and, therefore, are expected to be applicable to a wide range of applications, including this one. Since there are no universal model performance criteria for MB, MAE, and HR, we set the criteria as follows:

- air temperature: $|MB| \leq 0.5$ K, $MAE \leq 2$ K, and $HR \geq 90\%$
- dewpoint depression: $|MB| \leq 1$ K, $MAE \leq 2$ K, and $HR \geq 70\%$
- wind speed: $|MB| \leq 1$ m s^{-1}, $MAE \leq 2$ m s^{-1}, and $HR \geq 50\%$
- wind direction: $|MB| \leq 10°$, $MAE \leq 30°$, and $HR \geq 70\%$

Table 3 indicates that no single simulation provides the overall best or worst performance for all the near-surface fields considered in our work. This finding is consistent with that of Grimmond et al. (2010), which reports on an international effort to understand the complexity required to model the surface energy balance in urban areas. Grimmond et al. (2010) compared 33 urban energy balance models with varying degrees of complexity against site observations. One striking conclusion of this comparison is that, overall, the simpler models perform as well as the more complex models.

Generally, the simulations reproduce better 2-m temperature and dewpoint depression than 10-m wind speed and direction, for the criteria that we set in this work. The simpler urban parametrization schemes perform as well as the more sophisticated schemes when considering all the statistical metrics, whether all the sites, all the urban sites only, or all the rural sites only are considered. The only significant difference between the different schemes that can be identified in Table 3 is for wind speed in urban areas, for which BEP performs best. The wind speed in urban areas is overestimated when using the bulk urban parametrization scheme and SLUCM while it is slightly underestimated when using BEP. A similar finding was reported by Salamanca et al. (2011). This suggests that the drag effects of buildings are better captured with a multilayer (rather than single layer or bulk) urban canopy model. Interestingly, the inclusion of building anthropogenic fluxes in BEP + BEM does not improve overall model performance compared with BEP. This may be due to inappropriate default parameter values for BEM.

The categorization of the urban land cover, according to the fractional area that is built-up within each grid cell, improves the overall performance for SLUCM while it results in similar performance for BEP. When considering the urban sites for SLUCM, *HR* increases by approximately 9, 9, and 13% for 2-m temperature, 2-m dewpoint depression, and 10-m wind speed, respectively, while it decreases by less than 2% for 10-m wind direction (see Table 3). As part of the international urban energy balance model comparison, Grimmond et al. (2011) also reported that providing surface-cover fractions generally results in better performance, even though a poor choice of parameter values can affect dramatically the performance of models that otherwise perform well.

3.3 UHI intensity

The UHI intensity is calculated as the difference in 2-m temperature between Westminster - Marylebone Road and Wisley (see sites 1 and 11 in Fig. 2) at a given time. The site at Westminster - Marylebone Road is located in central London in a densely built-up area, which is categorized in the model as low-intensity residential (see Sect. 2). As for the site at Wisley, it is situated in a rural landscape, which is categorized in the model as crop land. Times series of observed and predicted UHI intensity are presented in Fig. 3, where the maximum observed UHI intensity is in the range 3 – 5 K. This range of values is similar to that reported for similar conditions and time of the year in London (Bohnenstengel et al. 2011) and other megacities, such as Paris, France (Sarkar and De Ridder 2011). The predicted UHI intensity has a similar temporal variability for all the model simulations (S1 to S7). Overall, the model simulations reproduce reasonably well the increase in the UHI intensity after sunset and its decrease before sunrise. There is no clear evidence that using a multilayer or single layer (rather than bulk) urban canopy model improves the representation of the intensity of the UHI. The categorization of the urban land cover, according to the fractional area that is built-up within each grid cell, leads to improved predictions of the UHI intensity.

The UHI intensity is underpredicted by the model by 2 – 3 K from 0300 to 0600 UTC on 7 May 2008 for all the model simulations. The predicted UHI intensity peaks at the same time as the observed UHI intensity. The predicted 2-m temperature at the rural site (Wisley) decreases by less than 1 K from 0300 to 0500 UTC, while its observed counterpart decreases by more than 2 K (not shown). From the model predictions and the limited observations available, there is no indication of any large-scale feature that could be the cause for this discrepancy. This positive 2-m temperature bias in the model during this period was found for only a few sites in low-lying rural areas. For these sites and during this period, the

observations indicate that the 2-m dewpoint depression was near to zero (i.e, the near-surface air was close to saturation). Since the sky was clear and the wind was light, it is probable that ground fog had formed. The predicted 2-m dewpoint depression was overestimated by about 1 K when compared to its observed counterpart. The discrepancies for the predicted 2-m temperature and dewpoint depression are likely to be the result of local subgrid-scale topographic effects, in relation to soil type, vegetation type and orography, that are not included in the model. Having said that, we cannot rule out the possible impact of the initial conditions for the soil moisture and temperature.

4 Effects of the marine air intrusion on London's UHI

A caveat is worth noting here. The model results discussed in Sect. 3 are inevitably limited to particular times and sites. It is difficult to assess thoroughly the generality of our results. Even though using a multilayer (rather than single layer or bulk) urban canopy model does not clearly improve the prediction of the intensity of the UHI, it does improve the prediction of its spatial pattern (i.e., similar performance for urban and rural sites) as can be seen in Table 3. Since BEP + BEM does not significantly improve results compared to using BEP alone, we focus our attention in the following to results of simulation S6 (CEH + IGBP/MODIS and BEP, see Table 2).

The time evolution of the spatial distribution of predicted and observed 2-m temperature in the subset of Domain 4 used for analysis of model results (see Fig. 1b) for simulation S6 (CEH + IGBP/MODIS and BEP, see Table 2) is presented on 7 May 2008 at 0900, 1200, 1500, 1800, and 2100 UTC in Fig. 4. The signature of London's UHI is clearly discernible, and predicted near-surface temperatures are in good agreement with their observed counterparts. Topographic influences are evident in Fig. 4, where air is cooler above the higher

orographic features than in the low-lying areas. Such thermal gradients induced by topographic effects in the London area were noted by Chandler (1962). The advection of cooler air from the North Sea reduces the intensity of the UHI in the windward suburbs and displaces it 5 to 10 km to the west, in good agreement with observations. The cooling effect of the marine air intrusion diminishes progressively over the course of the night. The thermal centre gradually shifts back toward the City of London borough shortly after midnight (not shown). A similar effect was reported by Gedzelman et al. (2003) for the UHI of New York City during strong sea breezes.

During this period of easterly winds, the airflow is channelled through the Weald, the North Downs and Medway Gap (see also Fig. 1b). During daytime, the air temperature rises more over land than over the sea. A baroclinic zone organized as a SBF develops at the transition between the continental and marine air masses. From 0900 to 1200 UTC, as the marine air penetrates inland toward the west-south-west sector, the SBF crosses the North Downs east of Medway Gap and interacts with the south-easterly flow, creating a convergence zone (perpendicular to the flow direction), which propagates westward. The air is lifted along the convergence line. This convergence line was also noted by Bohnenstengel et al. (2011) in a numerical simulation of London's UHI on that day.

A (passive) tracer was released within the first model layer above the ground surface to investigate the impact of the marine air intrusion on transport characteristics above London's atmosphere. It was initialized at the beginning of the model calculation with a zero mixing ratio everywhere in the atmosphere, except within the first model layer, where its volume mixing ratio was set to 1 ppbv. The time evolution of a west-east vertical cross-section of tracer volume mixing ratio across South London, just north of the North Downs (see Fig. 1b) is shown on 7 May 2008 at 0900, 1200, 1500, 1800 and 2100 UTC in Fig. 5.

At 0900 UTC, the tracer is mixed in the growing boundary layer over land. Over the sea, it is confined near the surface into a shallow density current. The leading edge of the density current (i.e., the SBF) is clearly visible, with a tilting of the isolines of virtual potential temperature. At 1200 UTC, the SBF is well developed. Values of the gradient Richardson number at the rear of the leading edge are less than the critical value of 0.25, the condition required for Kelvin-Helmoltz instabilities to develop (Drazin 1958). Even though the gradient Richardson number is required to be less than 0.25 for instabilities to develop, there is evidence that turbulence can exist up to a gradient Richardson number in the order of unity (e.g., Galperin et al. 2007). Kelvin-Helmoltz billows (KHBs) form at the upper boundary of the sea-breeze density current. Trailing KHBs are noticeable at 1200, 1500 and 1800 UTC. The existence of well-developed KHBs in the present case study is supported in the observational study of Plant and Keith (2007), which indicates that the formation of distinct KHBs is enhanced for propagation of the SBF with a tail wind and for strong ambient wind speeds.

The tracer is lifted by the SBF and vented out of the boundary layer into the free troposphere (see for instance Fig. 5d), where the tracer can be transported over long distances. The tracer lifted up by the SBF is also mixed by the KHBs seaward thereby increasing tracer volume mixing ratio above the sea-breeze density current. Cool air advection across London efficiently cleanses the urban area of tracer, increasing tracer concentration downwind.

The above description of the marine air intrusion event is the same for all the sensitivity simulations (S1 to S7). However, there are subtle differences related to different parametrizations of the urban canopy. As pointed out in Sect. 3, the predicted 10-m wind speed in urban areas tends to be overestimated, when compared to observations, for the simulations using the bulk urban parametrization scheme and SLUCM, while it is generally underestimated for the simulations using BEP. Times series of observed and predicted 10-m wind speed and

2-m temperature at London City (see site 22 in Fig. 2) are presented in Fig. 6. The predicted 10-m wind speed is systematically underestimated at this site when using BEP while it is reasonably well captured when using the bulk urban parametrization scheme and SLUCM. The understimation of the 10-m wind speed when using BEP is more pronounced during the marine air intrusion event when it reaches about 3 m s^{-1}. The differences in terms of predicted 2-m temperature between the simulations using different urban parametrization schemes, at this site, are not as marked as those for the 10-m wind speed. The predicted 2-m temperature is within 1 – 2 K of its observed counterpart for all the sensitivity simulations. Interestingly, the agreement remains good during the marine air intrusion event. This indicates that there is a delicate balance between the effects of thermal advection and urbanization on near-surface fields, which depend, inter alia, on the parametrization of the urban canopy and the urban land-cover distribution. A quantification of these effects requires a carefully designed idealized case study, which is kept in mind for future work. For instance, in order to quantify the effects of thermal advection, one could consider London as a series of strips perpendicular to the wind direction, and investigate the effects of sequentially replacing the strips at the upwind edge of the city by non-urban strips until it consists of only non-urban strips.

5 Concluding remarks

This modelling work documented the response of London's UHI to a marine air intrusion (including a sea-breeze front), in an easterly wind regime, for a case study of 7 May 2008. Simulations were performed with the WRF model, version 3.2.1, on multiple grids using one-way nesting with the innermost domain covering London and its rural surroundings with a horizontal grid resolution of 1 km.

A sensitivity study was undertaken to assess how the categorization of the urban land cover and the parametrization of the urban canopy in the WRF model affect its performance characteristics for the near-surface air temperature, dewpoint depression, and wind fields (see Sect. 3). It was demonstrated that the WRF model is capable of reproducing those fields with a horizontal grid resolution of 1 km, for this case study and at the locations of the considered monitoring sites. It was shown that no single simulation provides the overall best or worst performance for all the near-surface fields considered. The categorization of the urban land cover, according to the fractional area that is built-up within each grid cell, resulted in better performance for SLUCM and similar performance for BEP. Using a multilayer (rather than single layer or bulk) urban canopy model did not clearly improve the prediction of the intensity of the UHI. Having said that, it did improve the prediction of its spatial pattern (i.e., similar performance for urban and rural sites) as can be seen in Table 3. Providing surface-cover fractions led to improved predictions of the UHI intensity.

From our results, we clearly saw evidence of the interaction of the marine air intrusion, in an easterly wind regime, with London's UHI (see Sect. 4). This is a two-way interaction in the sense that the UHI acts to intensify the differential heating between the continental and marine air masses and thus the SBF. The advection of cooler air from the North Sea reduced the intensity of the UHI in the windward suburbs and displaced it 5 to 10 km to the west, in good agreement with observations. Frontal advection across London effectively replaced the air in the urban area as indicated by the tracer experiment. The redistribution of the tracer in the vertical did have a significant impact on near-surface concentration. SBFs may be an important contributor to boundary-layer ventilation in the London area. Marine air intrusions will also affect the behaviour of pollutants downwind, thereby impacting air quality (see also Miller et al. 2003). Results also indicated that there is a delicate balance between the effects of thermal advection and urbanization on near-surface fields, which

depend, inter alia, on the parametrization of the urban canopy and the urban land-cover distribution.

The UHI intensity varies seasonally, so it would be interesting to evaluate whether the model performs in a similar way for a contrasting winter case study. Further work will include a detailed comparison with field observations to be collected in 2012, such as the comparison by Lee et al. (2011).

Acknowledgements This study has been conducted as part of the Clean Air for London (ClearfLo) project, funded by the UK National Environment Research Council (NERC). The authors benefited from fruitful discussion with S. I. Bohnenstengel and Prof. S. E. Belcher. MIDAS data was provided by the UK Met Office through the British Atmospheric Data Centre (BADC).

References

Arnfield AJ (2003) Two decades of urban climate research: a review of turbulence, exchanges of energy and water, and the urban heat island. Int J Climatol 23:1–26

Arritt RW (1993) Effects of the large-scale flow on characteristics features of the sea breeze. J Appl Meteorol 32:116–125

Atkins NT, Wakimoto RM (1997) Influence of the synoptic-scale flow on sea breezes observed during CaPE. Mon Weather Rev 125:2112–2130

Bechtold P, Pinty JP, Mascart P (1991) A numerical investigation of the influence of large-scale winds on sea-breeze- and inland-breeze-type circulations. J Appl Meteorol 30:1268–1279

Bohnenstengel SI, Evans S, Clark PA, Belcher SE (2011) Simulations of the London urban heat island. Q J R Meteorol Soc 137:1625–1640

Bougeault P, Lacarrère P (1989) Parameterization of orography-induced turbulence in a mesobeta-scale model. Mon Weather Rev 117:1872–1290

Chandler TJ (1962) London's urban climate. Geogr J 128:279–298

Chen F, Dudhia J (2001) Coupling an advanced land-surface/hydrology model with the Penn State/NCAR MM5 modeling system. Part I: model implementation and sensitivity. Mon Weather Rev 129:569–585

448 Chen F, Kusaka H, Bornstein R, Ching J, Grimmond CSB, Grossman-Clarke S, Loridan T, Manning KW,
449 Martilli A, Miao S, Sailor D, Salamanca FP, Taha H, Tewari M, Wang X, Wyszogrodzki AA, Zhang C
450 (2011) The integrated WRF/urban modelling system: development, evaluation, and applications to urban
451 environmental problems. Int J Climatol 31:273–288
452 Cox R, Bauer BL, Smith T (1998) A mesoscale model intercomparison. Bull Am Meteorol Soc 79:265–283
453 Crosman ET, Horel JD (2010) Sea and lake breezes: a review of numerical studies. Boundary-Layer Meteorol
454 137:1–29
455 Damato F, Planchon O, Dubreuil V (2003) A remote-sensing study of the inland penetration of sea-breeze
456 fronts from the English Channel. Weather 58:219–226
457 Dandou A, Tombrou M, Soulakellis N (2009) The influence of the City of Athens on the evaluation of the sea
458 breeze front. Boundary-Layer Meteorol 131:35–51
459 Drazin PG (1958) The stability of a shear layer in an unbounded heterogeneous inviscid fluid. J Fluid Mech
460 4:214–224
461 Eastwood E, Rider GC (1961) A radar observation of a sea-breeze front. Nature 189:978–980
462 Estoque MA (1962) The sea breeze as a function of the prevailing synoptic situation. J Atmos Sci 19:244–250
463 Findlater J (1964) The sea-breeze and inland convection. Meteorol Mag 93:82–89
464 Freitas ED, Rozoff CM, Cotton WM, Silvia Dias PL (2007) Interactions of an urban heat island and sea
465 breeze circulations during winter over the metropolitan area of Sao Paulo. Boundary-Layer Meteorol
466 122:43–65
467 Galperin B, Sukoriansky S, Anderson PS (2007) On the critical Richardson number in stably stratified turbu-
468 lence. Atmos Sci Let 8:65–69
469 Gedzelman SD, Austin S, Cermak R, Stefano N, Partridge S, Quesenberry S, Robinson DA (2003) Mesoscale
470 aspects of the Urban Heat Island around New York City. Theor Appl Climatol 75:29–42
471 Gemmill W, Katz B, Li X (2007) Daily Real-Time Global Sea Surface Temperature - High-Resolution anal-
472 ysis: RTG_SST_HR. NCEP/EMC Office Note No. 260, NOAA/NCEP, Camp Springs, MD, USA, 39
473 pp.
474 Giridharan R, Kolokotroni M (2009) Urban heat island characteristics in london during winter. Sol Energy
475 83:1668–1682
476 Grell GA, Dévényi D (2002) A generalized approach to parameterizing convection combining ensemble and
477 data assimilation techniques. Geophys Res Lett 121:D14/1693

478 Grimmond CSB, Blackett M, Best MJ, Barlow J, 30 co-authors (2010) The international urban energy balance
479 models comparison project: first results from Phase 1. J Appl Meteorol Climatol 49:1268–1292
480 Grimmond CSB, Blackett M, Best MJ, 33 co-authors (2011) Initial results from Phase 2 of the international
481 urban energy balance model comparison. Int J Climatol 31:244–272
482 Iacono MJ, Delamere JS, Mlawer EJ, Shephard SA, Clough SA, Collins WD (2008) Radiative forcing
483 by long-lived greenhouse gases: Calculations with the AER radiative transfer models. J Geophys Res
484 113:D13,103, DOI 10.1029/2008JD009944
485 Kolokotroni M, Giridharan R (2008) Urban heat island intensity in London: An investigation of the impact of
486 physical characteristics on changes in outdoor air temperature during summer. Sol Energy 82:986–998
487 Kusaka H, Kimura F (2004) Coupling a single-layer urban canopy model with a simple atmospheric model:
488 impact on urban heat island simulation for an idealized case. J Meteorol Soc Jpn 82:67–80
489 Kusaka H, Kimura F, Hirakuchi H, Mizutori M (2000) The effects of land-use alteration on the sea breeze
490 and daytime heat island in the Tokyo metropolitan area. J Meteorol Soc Jpn 78:405–420
491 Kusaka H, Kondo H, Kikegawa Y, Kimura F (2001) A simple single-layer urban canopy model for atmo-
492 spheric models: comparison with multi-layer and slab models. Boundary-Layer Meteorol 101:329–358
493 Lee SH, Kim SW, Angevine WM, Bianco L, McKeen SA, Senff CJ, Trainer M, Tucker SC, Zamora RJ (2011)
494 Evaluation of urban surface parameterizations in the WRF model using measurements during the Texas
495 Air Quality Study 2006 field campaign. Atmos Chem Phys 11:2127–2143
496 Lemonsu A, Bastin S, Masson V, Drobinski P (2006) Vertical structure of the urban boundary layer over
497 Marseille under sea-breeze conditions. Boundary-Layer Meteorol 118:477–501
498 Liu Y, Chen F, Warner T, Basara J (2006) Verification of a mesoscale data-assimilation and forecasting system
499 for the Oklahoma City area during the Joint Urban 2003 field project. J Appl Meteorol Climatol 45:912–
500 929
501 Marshall WAL (1950) Sea-breeze across London. Meteorol Mag 79:165–168
502 Martilli A, Clappier A, Rotach MW (2002) An urban surface exchange parameterization for mesoscale mod-
503 els. Boundary-Layer Meteorol 104:261–304
504 Masson V (2006) Urban surface modeling and the meso-scale impact of cities. Theor Appl Climatol 84:35–45
505 Miller STK, Keim BD, Talbot RW, Mao H (2003) Sea breeze: Structure, forecasting, and impacts. Rev Geo-
506 phys 41:1011, DOI 10.1029/2003RG000124

507 Morrison H, Thompson G, Tatarskii V (2009) Impact of cloud microphysics on the development of trail-
508 ing stratiform precipitation in a simulated squall line: Comparison of one and two-moment schemes.
509 Mon Weather Rev 137:991–1006
510 Ohashi Y, Kida H (2002) Local circulations developed in the vicinity of both coastal and inland urban areas:
511 A numerical study with a mesoscale atmospheric model. J Appl Meteorol 41:30–45
512 Ohashi Y, Kida H (2004) Local circulations developed in the vicinity of both coastal and inland urban areas.
513 Part II: Effects of urban and mountain areas on moisture transport. J Appl Meteorol 43:119–133
514 Oke TR (1982) The energetic basis of the urban heat island. Q J R Meteorol Soc 108:1–24
515 Plant RS, Keith GJ (2007) Occurence of Kelvin-Helmholtz billows in sea-breeze circulations. Boundary-
516 Layer Meteorol 122:1–15
517 Rotach MW (1993) Turbulence close to a rough urban surface, Part II: Variances and gradients. Boundary-
518 Layer Meteorol 66:75–92
519 Salamanca F, Martilli A (2010) A new Building Energy Model couled with an Urban Canopy Parame-
520 terization for urban climate simulations – part II: Validation with one dimension off-line simulations.
521 Theor Appl Climatol 99:345–356
522 Salamanca F, Martilli A, Tewari M, Chen F (2011) A study of the urban boundary layer using different urban
523 parameterizations and high-resolution urban canopy parameters with wrf. J Appl Meteorol Climatol
524 50:1107–1128
525 Sarkar A, De Ridder K (2011) The urban heat island intensity of paris: a case study based on a simple urban
526 surface parametrization. Boundary-Layer Meteorol 138:511–520
527 Schlünzen KH, Sokhi RS (2008) Overview of tools and methods for meteorological and air pollution
528 mesoscale model evaluation and user training. Joint Report of COST Action 728 and GURME, GAW
529 Report No. 181, WMO/TD-No. 1457, WMO, Geneva, Switzerland, 121 pp.
530 Simpson JE, Mansfield DA, Milford JR (1977) Inland penetration of sea-breeze fronts. Q J R Meteorol Soc
531 103:47–76
532 Skamarock WC, Klemp JB, Dudhia J, Gill DO, Barker DM, Duda MG, Huang XY, Wang W, Powers JG
533 (2008) A description of the Advanced Research WRF Version 3. NCAR Technical Note NCAR/TN-
534 475+STR, NCAR, Boulder, CO, USA, 125 pp.
535 Stauffer DR, Seaman N (1990) Use of Four-Dimensional Data Assimilation in a limited-area mesoscale
536 model. Part I: Experiments with synoptic-scale data. Mon Weather Rev 118:1250–1277

Sumner GN (1977) Sea breeze occurrence in hilly terrain. Weather 32:200–208

Thompson WT, Holt T, Pullen J (2007) Investigation of a sea breeze front in an urban environment. Q J R Meteorol Soc 133:579–594

UK Meteorological Office (2006) MIDAS Land Surface Stations data (1853–current). NCAS British Atmospheric Data Centre. http://badc.nerc.ac.uk/view/badc.nerc.ac.uk__ATOM__dataent_ukmo-midas. Accessed 2 February 2012

Watkins R, Palmer J, Kolokotroni M, Littlefair P (2002) The London Heat Island: results from summertime monitoring. Build Serv Eng Res Technol 23:97–106

Yoshikado H (1990) Vertical structure of the sea breeze penetrating through a large urban complex. J Appl Meteorol 29:878–891

Yoshikado H (1992) Numerical study of the daytime urban effect and its interaction with the sea breeze. J Appl Meteorol 31:1146–1164

Zhong S, Takle ES (1993) The effects of large-scale winds on the sea-land-breeze circulations in an area of complex coastal heating. J Appl Meteorol 32:1181–1195

List of Figures

Tables

Table 1 Spatial coverage and horizontal resolution of the grids used for the simulations

Domain	Typical extent	Grid points (E-W × N-S)	Grid size (km)
Domain 1	North Atlantic, Europe, and North Africa	192 × 128	48
Domain 2	Europe	321 × 257	12
Domain 3	UK and Republic of Ireland	256 × 256	4
Domain 4	South-east England	257 × 257	1

Table 2 Description of the simulations used for the sensitivity experiments

Run	Land-cover dataset	Urban parametrization scheme
S1	IGBP/MODIS	Bulk parametrization
S2	IGBP/MODIS	SLUCM
S3	IGBP/MODIS	BEP
S4	IGBP/MODIS	BEP + BEM
S5	CEH + IGBP/MODIS	SLUCM
S6	CEH + IGBP/MODIS	BEP
S7	CEH + IGBP/MODIS	BEP + BEM

Table 3 Domain-wide statistics for hourly mean near-surface fields (2-m temperature, 2-m dewpoint depression, 10-m wind speed, and 10-m wind direction), considering all predicted/observed pairs of values from the sites reported in Fig. 2 for the period from 6 May 2008 at 1800 UTC to 8 May 2008 at 0600 UTC. The statistical metrics that are reported here, and defined in the text, namely mean bias (*MB*), mean absolute error (*MAE*) and hit rate (*HR*), are given for the simulations S1 to S7 (see text), considering all the sites, all the urban sites only, and all the rural sites only. The values that are reported in bold font do not fulfill the performance criteria set in Sect. 3.2

2-m temperature

Run	*MB* (K)			*MAE* (K)			*HR* (%)		
	All	Urban	Rural	All	Urban	Rural	All	Urban	Rural
S1	0.21	0.07	0.50	0.81	0.80	0.95	93.97	95.48	**89.45**
S2	−0.39	**−0.89**	0.05	0.95	1.29	0.92	**89.95**	**83.42**	**87.94**
S3	0.05	−0.37	0.37	0.80	0.91	0.90	93.97	92.46	90.96
S4	0.07	−0.30	0.40	0.80	0.88	0.91	93.97	91.96	90.96
S5	−0.29	−0.43	0.17	0.93	1.06	0.95	**89.95**	92.46	**85.43**
S6	0.19	0.20	0.44	0.81	0.81	0.94	94.47	94.47	**89.45**
S7	0.22	0.27	0.46	0.83	0.83	0.96	93.47	92.97	**89.45**

2-m dewpoint depression

Run	*MB* (K)			*MAE* (K)			*HR* (%)		
	All	Urban	Rural	All	Urban	Rural	All	Urban	Rural
S1	0.67	0.93	0.64	1.46	1.84	1.35	73.87	**63.82**	77.39
S2	−0.09	−0.84	0.14	1.22	1.62	1.17	80.91	70.85	79.90
S3	0.45	−0.29	0.49	1.34	1.62	1.26	76.88	73.37	78.39
S4	0.47	−0.19	0.51	1.36	1.63	1.28	75.38	72.86	77.39
S5	0.04	−0.28	0.24	1.23	1.40	1.19	79.90	79.90	78.89
S6	0.62	0.39	0.56	1.41	1.60	1.28	74.87	71.86	79.40
S7	0.65	0.46	0.58	1.45	1.63	1.30	73.87	71.86	78.89

10-m wind speed

Run	*MB* (K)			*MAE* (K)			*HR* (%)		
	All	Urban	Rural	All	Urban	Rural	All	Urban	Rural
S1	**2.05**	**2.47**	**1.63**	**2.36**	**2.64**	1.94	**16.08**	**17.09**	**23.62**
S2	**1.76**	**1.82**	**1.54**	**2.12**	**2.12**	1.90	**21.61**	**22.61**	**25.13**
S3	**1.28**	−0.01	**1.59**	1.75	1.30	1.90	**28.64**	**46.23**	**25.63**
S4	**1.28**	0.01	**1.59**	1.75	1.29	1.91	**28.14**	**46.23**	**25.13**
S5	**1.77**	**1.34**	**1.53**	**2.13**	1.78	1.89	**22.11**	**35.18**	**26.63**
S6	**1.11**	−0.44	**1.55**	1.68	1.38	1.87	**33.17**	**42.71**	**29.65**
S7	**1.12**	−0.42	**1.55**	1.68	1.38	1.87	**32.66**	**42.21**	**29.65**

10-m wind direction

Run	*MB* (K)			*MAE* (K)			*HR* (%)		
	All	Urban	Rural	All	Urban	Rural	All	Urban	Rural
S1	−6.26	2.59	**−11.62**	27.64	26.79	**38.93**	84.42	81.91	76.38
S2	−4.06	1.99	−4.10	26.33	27.88	**35.48**	84.42	79.90	75.88
S3	−8.29	−0.21	**−12.44**	27.31	26.47	**38.57**	84.42	70.90	76.38
S4	−8.19	0.08	**−12.37**	27.30	26.46	**38.58**	84.42	79.90	76.38
S5	−2.26	−5.45	0.09	25.18	**35.80**	29.33	85.43	78.39	76.88
S6	−8.52	**−15.64**	−1.67	27.33	**38.47**	**30.34**	84.42	76.88	76.88
S7	−8.40	**−15.39**	−1.64	27.35	**38.47**	**30.40**	84.93	77.39	76.88

Figures

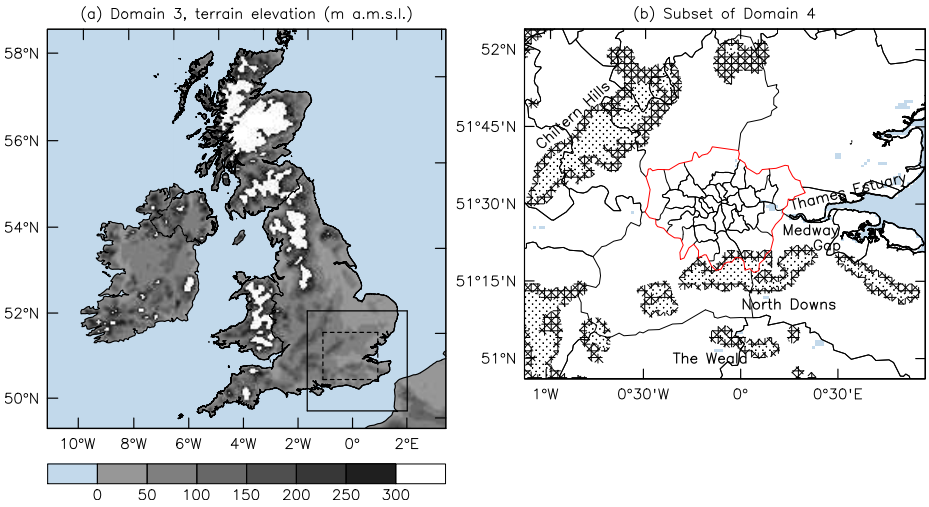

Fig. 1 **(a)** Orography of Domain 3 (see the text and Table 1). The solid and dashed polylines represent the areas of Domain 4 and a subset of it (see plot b), respectively. **(b)** Subset of Domain 4 used for analysis of model results. The polylines delineate the administrative areas. The red polyline represents the Greater London area, which encompasses the City of London and the London boroughs. Orographic features are shown using contours with shaded patterns (hashed- and stipple-filled patterns for terrain elevation greater than 100 and 150 m a.m.s.l., respectively)

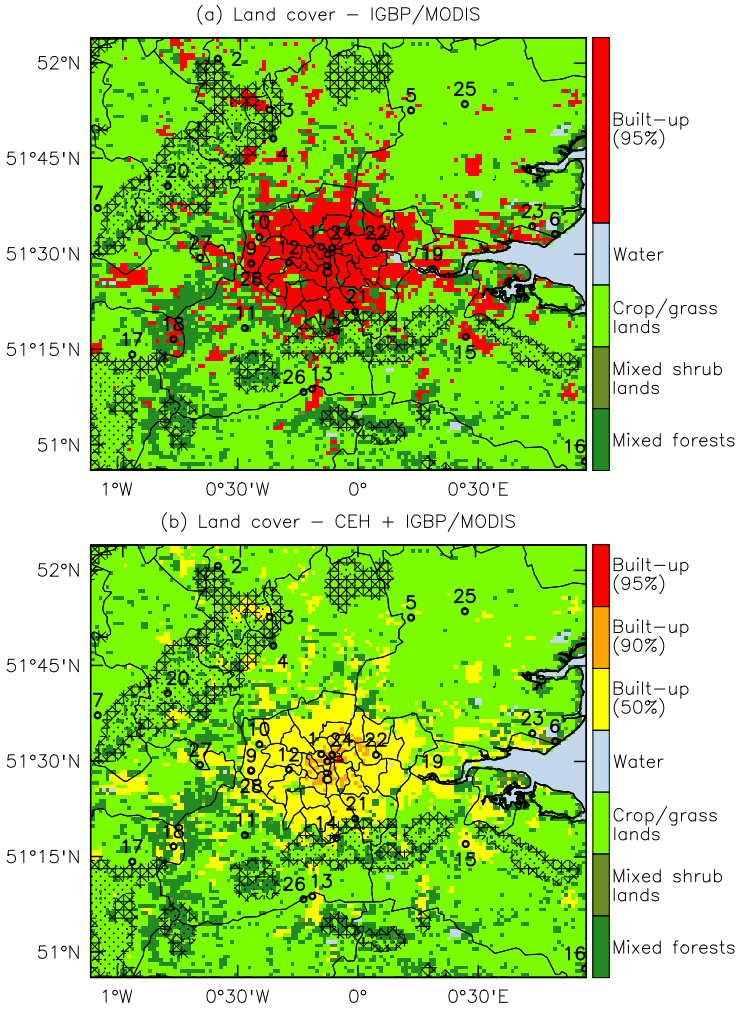

Fig. 2 Spatial distribution of the dominant land-cover type in the subset of Domain 4 used for analysis of model results (see Fig. 1b) for **(a)** the IGBP/MODIS dataset and **(b)** the CEH + IGBP/MODIS dataset. The monitoring sites used for the model evaluation presented in Sect. 3 are indicated by open circles: 1 – Westminster - Marylebone Road, 2 – Woburn, 3 – Luton, 4 – Rothamsted, 5 – Stansted, 6 – Shoeburyness, Landwick, 7 – Benson, 8 – St Jamess Park, 9 – Heathrow, 10 – Northolt, 11 – Wisley, 12 – Kew (Royal Botanic Gardens), 13 – Gatwick, 14 – Kenley Airfield, 15 – East Malling, 16 – Lydd-Ashford Airport, 17 – Odiham, 18 – South Farnborough, 19 – Gravesend, Broadness, 20 – High Wycombe HQSTC, 21 – Biggin Hill, 22 – London City, 23 – Southend Airport, 24 – London Weather Centre, 25 – Andrewsfield, 26 – Charlwood, 27 – Eton Dorney, and 28 – Heathrow2 (see text for details). The polylines delineate the administrative areas. Orographic features are shown using contours with shaded patterns (hashed- and stipple-filled patterns for terrain elevation greater than 100 and 150 m a.m.s.l., respectively)

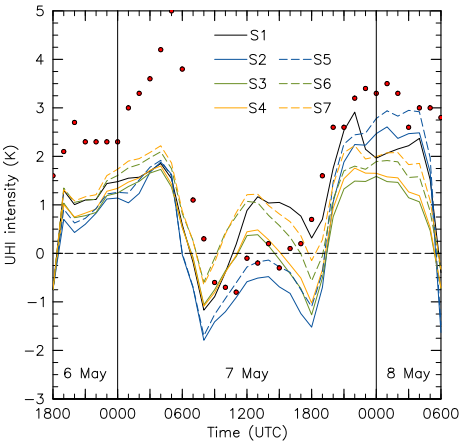

Fig. 3 Time series of observed (• symbols) and predicted (solid/dashed lines) urban heat island (UHI) intensity, defined as the difference in 2-m temperature between Westminster - Marylebone Road and Wisley (see sites 1 and 11 in Fig. 2) at a given time, for the simulations S1 to S7 (see Table 2) for the period from 6 May 2008 at 1800 UTC to 8 May 2008 at 0600 UTC

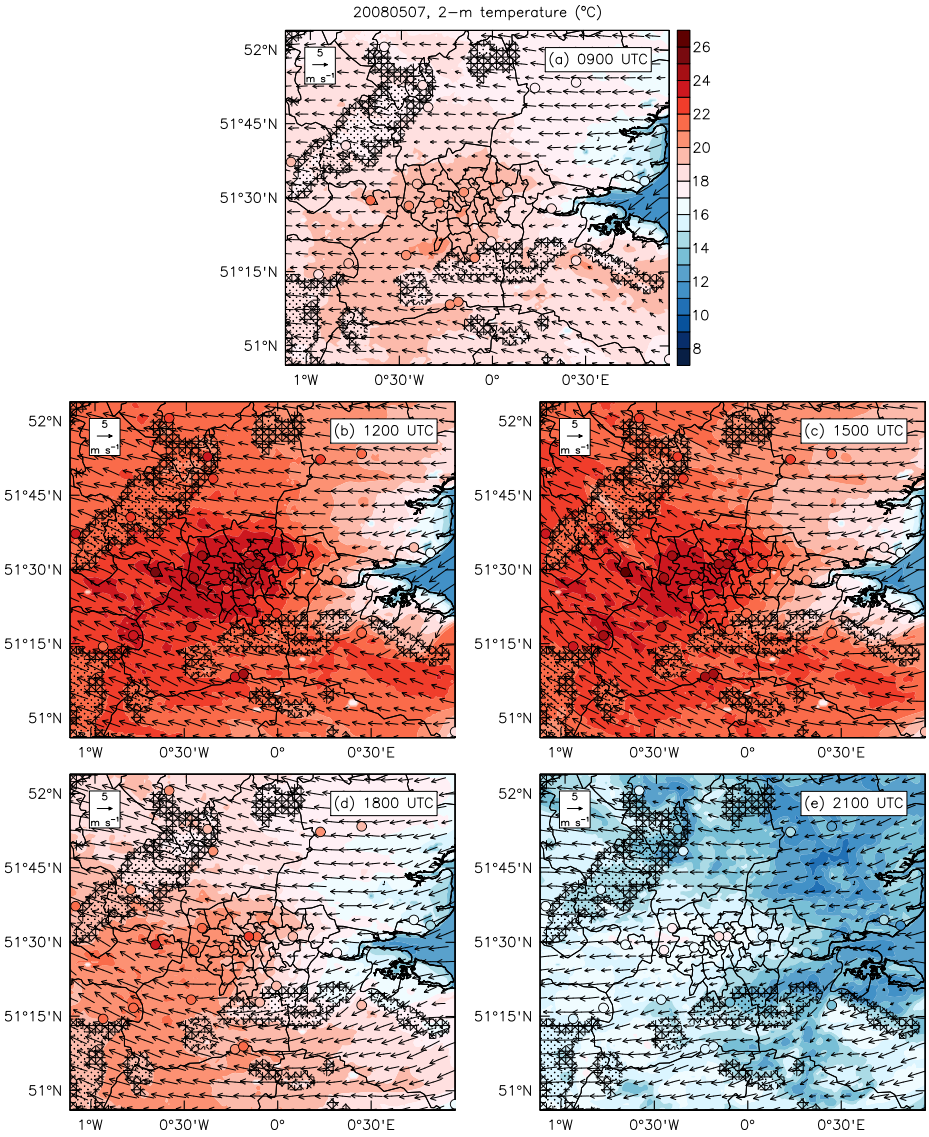

Fig. 4 Spatial distribution of the predicted 2-m temperature in the subset of Domain 4 used for analysis of model results (see Fig. 1b) for simulation S6 (CEH + IGBP/MODIS and BEP, see Table 2) on 7 May 2008 at **(a)** 0900 UTC, **(b)** 1200 UTC, **(c)** 1500 UTC, **(d)** 1800 UTC and **(e)** 2100 UTC. The observed 2-m temperatures from the monitoring sites used for the model evaluation presented in Sect. 3 (see Fig. 2) are reported as filled circles. Predicted 10-m horizontal wind vectors are superimposed. The polylines delineate the administrative areas. Orographic features are shown using contours with shaded patterns (hashed- and stipple-filled patterns for terrain elevation greater than 100 and 150 m a.m.s.l., respectively)

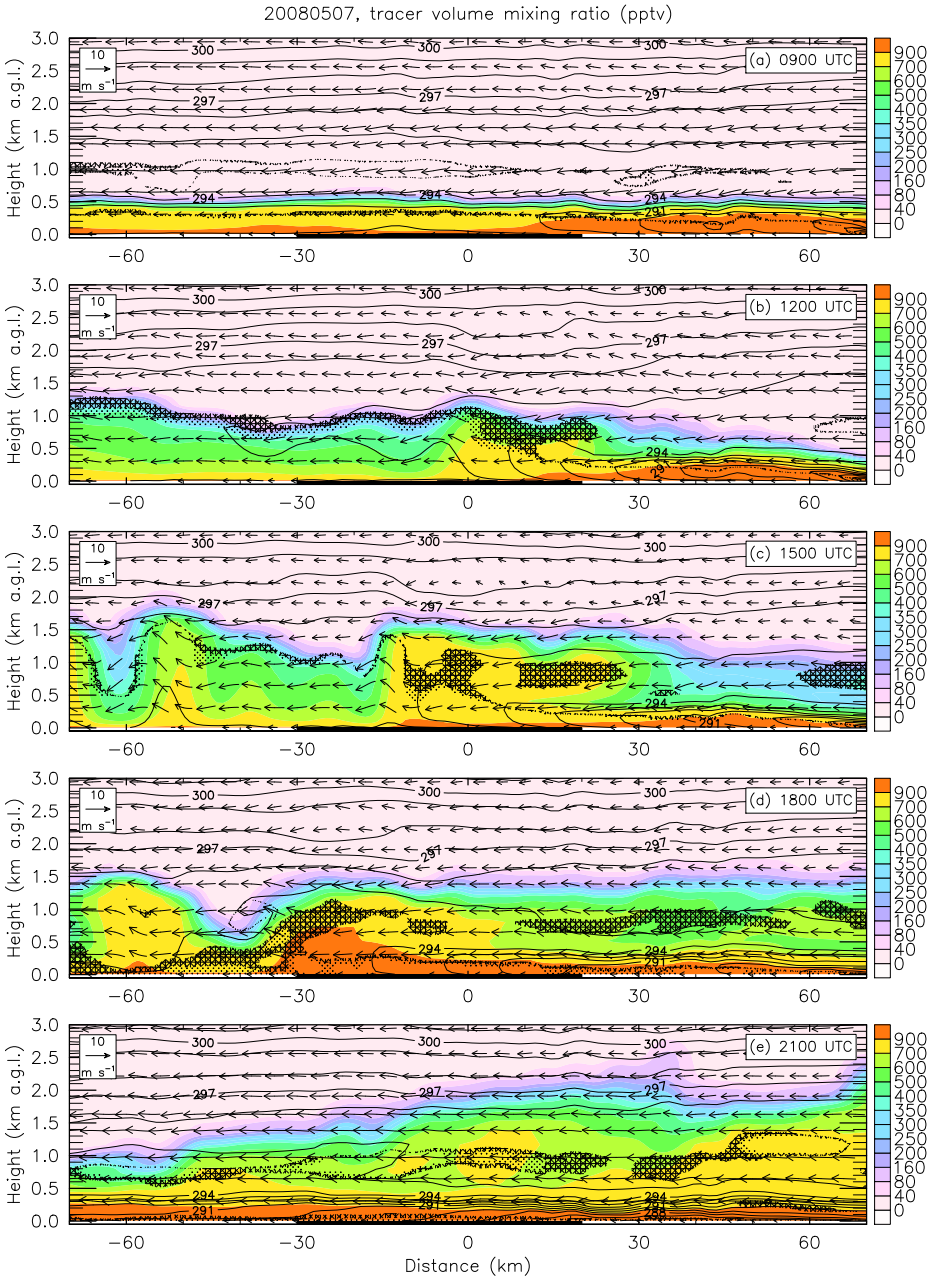

Fig. 5 West-east vertical cross-section of tracer volume mixing ratio across South London, just north of the North Downs (see Fig. 1b), for simulation S6 (CEH + IGBP/MODIS and BEP, see Table 2) on 7 May 2008 at **(a)** 0900 UTC, **(b)** 1200 UTC, **(c)** 1500 UTC, **(d)** 1800 UTC and **(e)** 2100 UTC. Predicted two-dimensional wind vectors in that vertical cross-section are superimposed. Isolines of virtual potential temperature are indicated as solid lines with 1 K interval contours. Richardson number values are shown using contours with shaded patterns (hashed- and stipple-filled for values lesser than 0.5 and 0.25, respectively). The black strip along the ground surface indicates the urban area of London

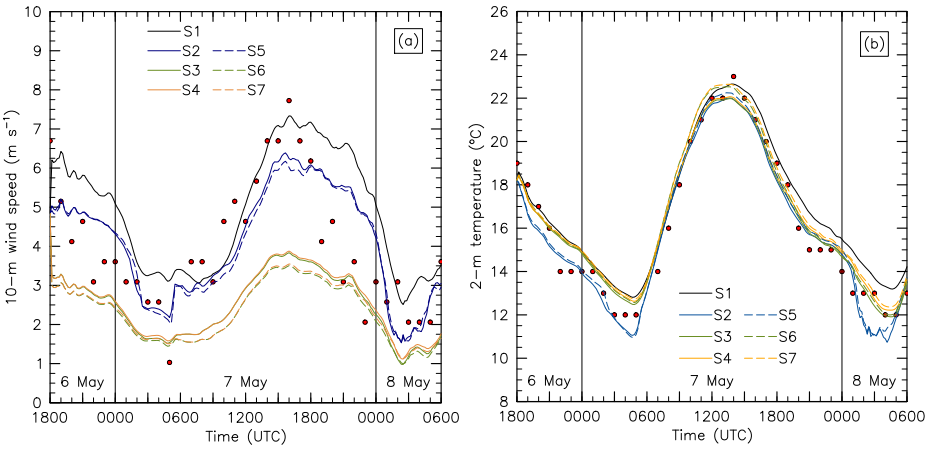

Fig. 6 Time series of observed (• symbols) and predicted (solid/dashed lines) 10-m wind speed **(a)** and 2-m temperature **(b)** at London City (see site 22 in Fig. 2), for the simulations S1 to S7 (see Table 2) for the period from 6 May 2008 at 1800 UTC to 8 May 2008 at 0600 UTC